Tropical Cyclone Motion and Surrounding Parameter Relationships

JOHN E. GEORGE[1] AND WILLIAM M. GRAY

Department of Atmospheric Science, Colorado State University, Ft. Collins 80523

(Manuscript received 29 January 1976, in revised form 28 October 1976

ABSTRACT

Ten years of rawinsonde data for 30 stations in the western North Pacific have been composited relative to tropical cyclone center positions. This information is used to study tropical cyclone motion and surrounding parameter relationships. Tropical cyclone motion and lower troposphere surrounding actual and geostrophic flow fields from 1°–7° radius are very well correlated. This general correlation of surrounding flow features applies equally well for cyclones with different directions of motion, speeds of propagation, intensities and intensity changes. The 700 mb level best specifies cyclone speed. The 500 mb level best specifies cyclone direction. The steering flow concept of cyclone motion appears to be quite valid in the statistical sense. These results may be useful to tropical cyclone forecasters.

1. Introduction

One of the most challenging problems in tropical meteorology is that of forecasting the movement of tropical cyclones. The relation of tropical cyclone movement to its surrounding flow has been previously examined by a number of meteorologists, but their data sources have usually been limited. The exact relation of cyclone movement to the surrounding flow has yet to be quantitatively established. Because tropical cyclones can be so devastating, it is important to try to better understand their movement so that improved forecasts can be made. With all the concentrated research and sophisticated forecasting techniques, the 24 h prediction error of the National Hurricane Center (Atlantic) and the Joint Typhoon Warning Center (Pacific) remains at 100–125 n mi. Vector forecast errors for 48 and 72 h are approximately 250 and 375 n mi, respectively. Because the 24 h forecast is the most critical in terms of lives and dollars, it is imperative that more research be attempted to improve this forecast. This may be possible by a more thorough quantitative investigation of cyclone motion and environment parameter relationships. This has been the purpose for this research.

2. Background

Tropical cyclone prediction methods can be classified in four categories:

1) Steering flow track prediction
2) Statistical track prediction
3) Numerical track prediction
4) Climatology-persistence track prediction.

The steering concept hypothesizes that tropical cyclones are vortices embedded in the basic environmental flow and should thus move with the so called "steering current." This is an established forecasting concept. The statistical forecast approach numerically screens various meteorological parameters for motion-related correlations and then uses these correlations to develop regression prediction equations. The numerical method uses primitive equation model prediction of the large-scale flow surrounding the cyclone and more recently a crude simulation of storm structure to dictate its future track. Climatology and/or persistence of storm track relies upon empirical relationships related to the cyclone tracks of previous storms.

Many objective schemes for tropical cyclone forecasting have been developed using one or more of the above prediction methods (see bibliography). Combining all schemes and systems, it can be stated that no one objective technique is superior at all times to another. There is no agreement on a specific outer steering current, although the majority of the schemes use lower tropospheric data. Some schemes work well for one storm, but poorly for another. The final forecast at the National Hurricane Center (Atlantic) and the Joint Typhoon Warning Center (JTWC) is a result of subjective modification of the multiple objective schemes. Although there has been improvement in the 48–72 h forecast time frame, significant improvement of the 24–36 h forecast has remained difficult to accomplish. This must be attributed to a basic lack of knowledge of the cyclone in its relation to its immediate environment and perhaps more importantly to the accuracy of measuring this environment.

With the recent availability of massive computer tape data storage, these data limitations can now be

[1] Capt. USAF. Present Affiliation: U. S. Air Force Global Weather Center, Offutt AFB, Neb. 68113.

partially overcome. This study is so directed. It employs 10 years of rawinsonde data around tropical cyclones in the western North Pacific. The mean composite surrounding winds are examined in relation to the cyclone motion. This is done at all levels in the atmosphere as well as for various radial distances from the cyclone center. Another unique feature of this study is that the data set is broken down into a group of subsets or stratifications based on certain characteristics of the cyclones. This is done on the hypothesis that if, indeed, there are certain steering relationships between the cyclone motion and the surrounding wind flow, then these relationships should be consistent regardless of different storm characteristics such as speed, direction of movement, intensity, etc. With the abovementioned amount of data and the stratification approach, this composite study does indeed describe consistent relationships between the cyclone motion and the surrounding flow. It is concluded that a new operational forecast scheme might be developed using the findings of this study with some possible improvement in track forecasting.

3. Data set and composite analysis

a. Compositing philosophy

The merit and requirement of rawinsonde compositing have been discussed previously by Williams and Gray (1973) and Ruprecht and Gray (1974). Basically, at one time period there are simply too few rawinsonde stations in proximity to a tropical cyclone to give enough data for a reasonably accurate surrounding analysis. This is true for all cyclone regions except possibly within the West Indies network. In the western North Pacific there is one region with many typhoons where no rawinsonde station is available within a 600 n mi radius circle. The surrounding observations that are available at regular time intervals are often not representative of the inner cyclone circulation. By compositing the rawinsondes from many cyclones with similar characteristics over many parts of the ocean, many of these data limitations can be overcome and the basic physical processes and relationships involved with the tropical storm better understood.

b. Data composite technique

The data used in this composite study come from 10 years of rawinsonde reports (1961–70) in the western North Pacific. The cyclone track data were obtained from the Guam JTWC best-track information. Fig. 1 shows the locations of the 30 stations available for that period. The western North Pacific has approximately 20 typhoons per year. Thus, over a 10-year period, there are approximately 200 typhoons. If each storm has approximately 6 days or 12 time periods of observations and 8 rawinsonde stations surrounding it at each time period (within 25° radius), then over a 10-year period approximately 20 000 rawinsonde reports are available for the entire data set. Within 15° radius there are about 9000 reports available around the storms as shown in Fig. 2. As can be seen for the complete data set, *the azimuthal distribution of rawinsonde reports is quite symmetrical at radii greater than 1°, and the number of rawinsonde reports in each outer averaging area is quite large.*

A 15° radius circular grid is used for the com-

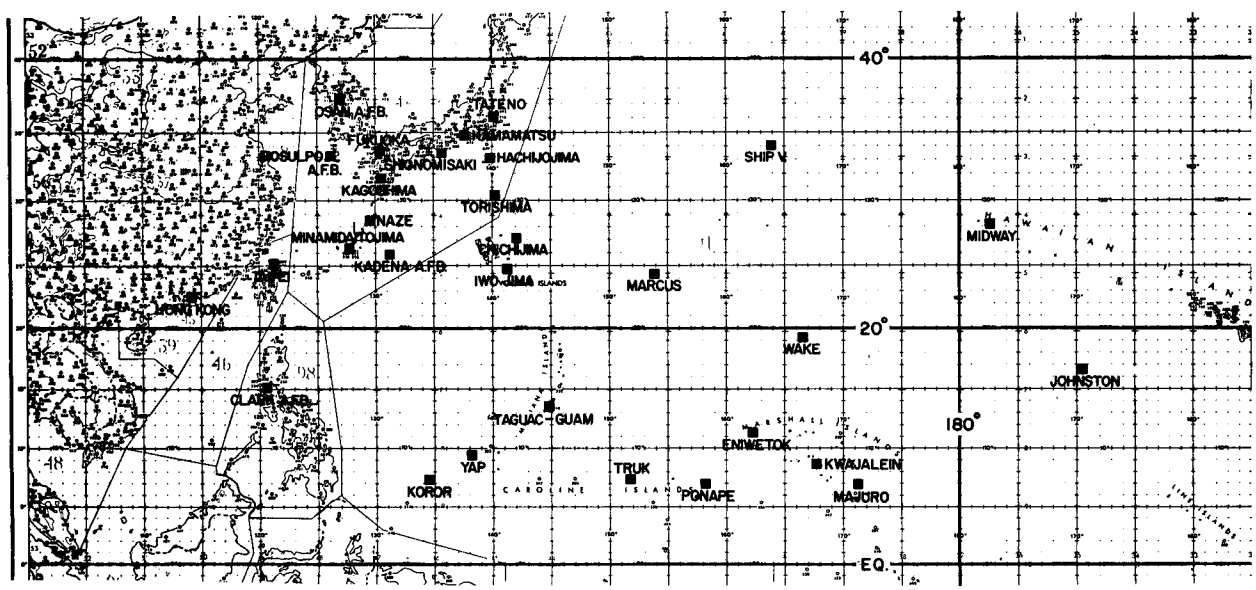

FIG. 1. Western North Pacific rawinsonde stations.

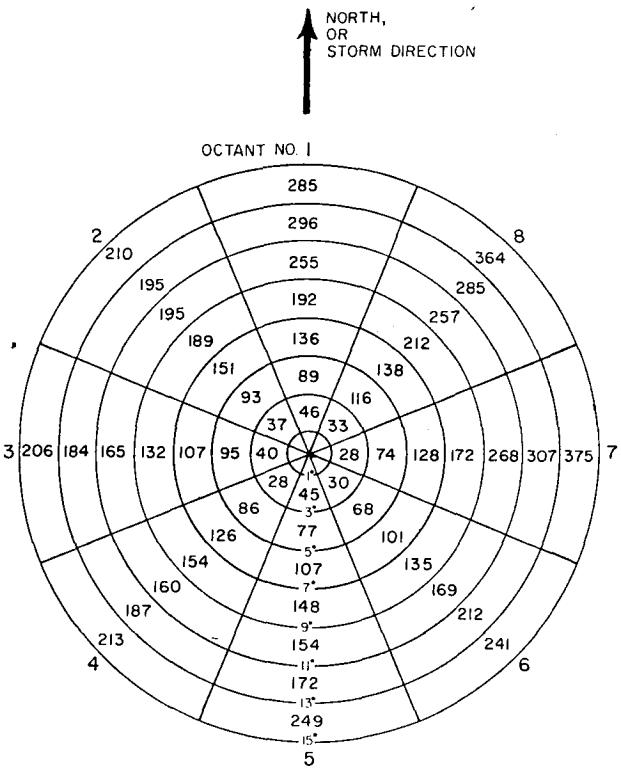

FIG. 2. Compositing grid (15° latitude radius) with the number of rawinsonde reports in each octant for the combined data set.

positing (see Fig. 2). Each sounding for each storm is recorded by latitude and longitude for each time period. Each sounding's position relative to the cyclone center (center of the grid) is then determined in cylindrical coordinates. All of the parameters to be composited, whether directly measured or computed from the directly measured parameters, are determined at the station locations at 19 levels from the surface to 50 mb.

The cylindrical grid consists of eight equal octants of 45° azimuth and eight radial annualar zones extending from 0°–1°, 1°–3°, 3°–5°, 5°–7°, 7°–9°, 9°–11°, 11°–13°, 13°–15°. These divide the grid into annular segments of various sizes. After all parameters have been measured or computed for each sounding, the value of each parameter is assigned to a point at the geometrical center of the individual grid space in which it falls. All soundings falling in that grid space for the particular group of storms and time periods being analyzed are then averaged or composited.

To obtain the best possible wind statistics each position of the moving storm and the ascending balloon at each level is recomputed in the following manner. The initial position of the storm is moved back along its motion vector a distance equal to 30 min travel according to its previous 12 h mean speed and direction of motion. This approximately corrects the storm position to its location at actual balloon release time as estimated from individual sounding reports. A mean balloon ascent rate of 5 m s^{-1} is assumed, and a mean ascent time to each of the upper pressure levels is computed. The position of the storm changes according to the assumed balloon ascent time to that level.

Using the same computed ascent times, the position of the balloon is changed at each level. For each ascent interval mean u and v wind components are computed and the balloon position is corrected by

$$\Delta X_i = \bar{u}_i \Delta t_i,$$
$$\Delta Y_i = \bar{v}_i \Delta t_i.$$

Therefore, the balloon position for each sounding changes at each level according to the observed winds.

c. *Data portrayal*

The above rawinsonde information is portrayed in a cylindrical coordinate system relative to the cyclone centers. Four separate reference frames can be used:

1) With respect to the instantaneously fixed cyclone center in a N–S or geographical coordinate system.
2) With respect to the cyclone center in a geographical coordinate system with the cyclone motion subtracted out of all the winds (portrayal of data relative to the moving cyclone center in geographical coordinates).
3) With respect to the instantaneously fixed cyclone center and the direction to which the storm is moving.
4) With respect to the cyclone center and the direction to which the storm is moving with the cyclone motion subtracted out of all the winds (portrayal of data relative to the cyclone center in a reference frame aligned according to the direction toward which the storm is moving).

This study employed the latter two compositing frames.

Information is portrayed at the following pressure levels: the surface, 1000, 950, 900, 850, 800, 700, 600, 500, 400, 300, 250, 200, 150, 100, 80, 70, 60 and 50 mb.

d. *Parameters composited*

The following parameters are measured or computed at each level in each coordinate system for each sounding:

Wind parameters	Thermodynamic parameters
u (zonal wind)	H (height)
v (meridional wind)	T (temperature)
v_θ (tangential wind)	
V (total wind).	

These parameters are composited at each of the 64 grid spaces at each level.

e. Storm motion[2] analysis coordinate system

From the basic coordinate systems described above the following storm motion coordinate system was devised for this study. The grid (see Fig. 2) is rotated to the direction of the cyclone motion so that in the compositing technique the cyclone motion is always at a zero or a 360° heading. From the data sample in the two relevant grids (stationary and moving as described in subsections 3c3 and 3c4), two surrounding center wind vectors at each of the 64 grid points were defined and calculated. These vectors are defined as the wind components perpendicular (V_N) and parallel (V_L) to the cyclone motion. The two component vectors of an example wind vector relative to the cyclone are shown in Fig. 3. From these data samples, an analysis was performed to determine the relationships between the surrounding wind flow direction and speed and the cyclone's motion. As previously stated, the data were broken down into a group of subsets or stratifications in order to detect differences, if any, in the storm motion-surrounding wind relationship for different storm characteristics. Table 1 lists the stratifications which were made.

f. Definitions

To better clarify how these composites were made, the following definitions are introduced:

(i) ROTated coordinate system (ROT)—Stationary grid aligned along the direction of the storm motion (coordinate grid is pointing in the direction of the storm motion). This system depicts the actual winds along and normal to the fixed cyclone center.

(ii) MOTion and ROTated coordinate system (MOTROT)—Same as the ROT system of (i) except the storm motion is vectorially subtracted from all the actual winds. Thus, wind components are portrayed along and normal to the moving storm position.

(iii) V_N—The wind component vector normal to the storm motion vector in the ROT system. (Positive to the right, negative to the left, looking in the direction to which the storm is moving.)

(iv) V_L—The wind component vector parallel to the storm motion in the ROT system. [Positive to the direction to which the storm moves (forward), negative opposite to which the storm moves (rear).]

(v) V_{NR}—Same as (iii) except in the MOTROT system.

(vi) V_{LR}—Same as (iv) except in the MOTROT system.

[2] Throughout this paper storm motion refers to the motion of the cyclone center.

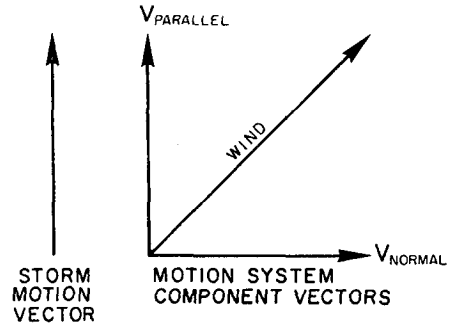

FIG. 3. Parallel and perpendicular components of a wind vector showing their relation to the storm motion vector.

(vii) Annular band—The horizontal average of the eight octant values of the grid for a single band, i.e., the 1°–3° radius band averaged around the storm for a single level.

(viii) Vertical annular band—Horizontal radial bands vertically integrated with respect to pressure levels, i.e., the 1°–3° averaged band integrated from 1000 to 100 mb, etc.

(ix) Horizontal multiple annular band—An area-weighted average for two or more horizontal radial bands, i.e., the 1°–7° radius band.

(x) Vertical multiple annular band—Multiple radial bands integrated with respect to pressure levels, i.e., the 1°–7° area-weighted radius band integrated from 1000 mb to 100 mb.

TABLE 1. Stratifications.

1. Lat>20°N	All storms with a latitude position greater than 20°N.
2. Lat<20°N	All storms with a latitude position less than 20°N.
3. Slow	Speed category for storms moving with a speed between 0 and 3 m s^{-1}.
4. Moderate	Speed category for storms moving with a speed between 4 and 7 m s^{-1}.
5. Fast	Speed category for storms moving with a speed greater than 7 m s^{-1}.
6. Direction A	Direction category for storms moving between 250° and 310°.
7. Direction B	Direction category for storms moving between 310° and 350°.
8. Direction C	Direction category for storms moving between 350° and 060°.
9. Intensity 1	Intensity category for storms with central pressures between 1000 mb and 980 mb.
10. Intensity 2	Intensity category for storms with central pressures between 980 mb and 950 mb.
11. Intensity 3	Intensity category for storms with central pressures less than 950 mb.
12. Deepening	Intensity change category for storms whose central pressures were decreasing at the time of observation.
13. Filling	Intensity change category for storms whose central pressures were increasing at the time of observation.

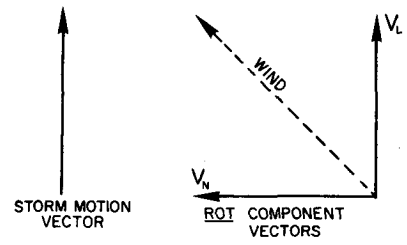

FIG. 4. Relation between component vectors V_L and V_N to the storm motion (ROT system).

The relation between the four component vectors (iii)–(vi) above is described below. Fig. 4 depicts the relation between the storm motion and the two component vectors of a wind in the ROT system. Fig. 5 depicts the subtraction of the storm motion vector which gives the new component V_{LR}. The normal component (V_N) is not affected by the subtraction since the grid is always aligned along the storm motion. The magnitude of V_N and V_{NR} are thus the same. For the parallel component in the MOTROT system (V_{LR})

$$V_{LR}+S_M=V_L,$$

where S_M is the magnitude of the storm motion.

4. Motion composite results

a. Storm asymmetry

It has long been known that the winds around a typhoon are not symmetrical. The right quadrant winds are typically stronger than the left quadrant. In order to examine the asymmetry of the composited data set, the right octant winds were compared with those of the left octant. The results at 700 mb for storms at latitudes greater and less than 20°N are portrayed in Figs. 6 and 7, respectively. Inside 1° radius the multiple hurricane flight data of Shea and Gray (1973) was added to the data sample. This asymmetry is typical for the other stratifications based on storm speed, direction, intensity and intensity change. Cyclone asymmetry is greatest at the radius of maximum winds which is located $\sim\frac{1}{3}°$ radius

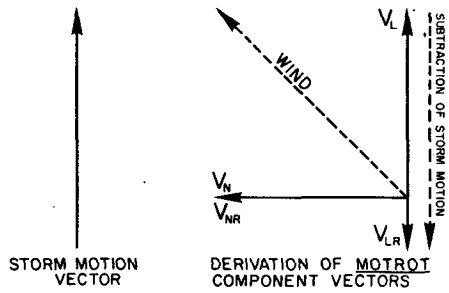

FIG. 5. Derivation of relative component vectors V_{LR} and V_{NR} for the MOTROT system. Note that V_N and V_{NR} are identical.

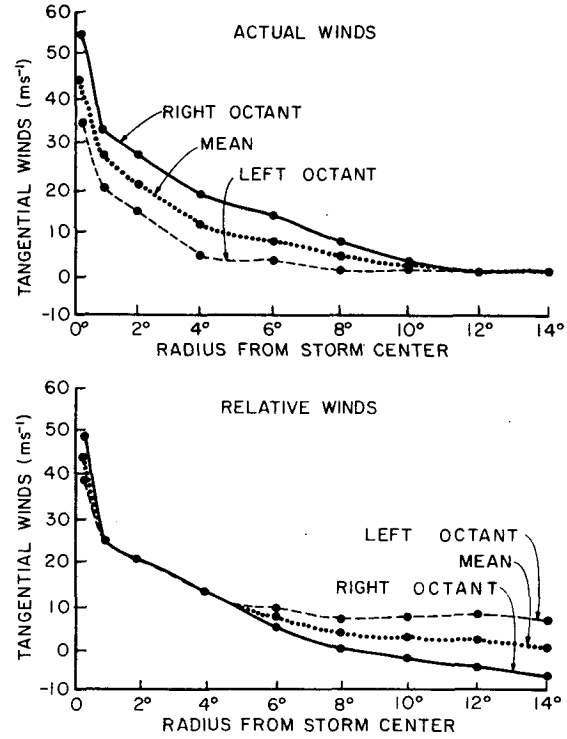

FIG. 6. 700 mb tangential wind profiles of actual and relative winds depicting the asymmetry between the right and left octants of tropical cyclones for the Lat>20°N stratification.

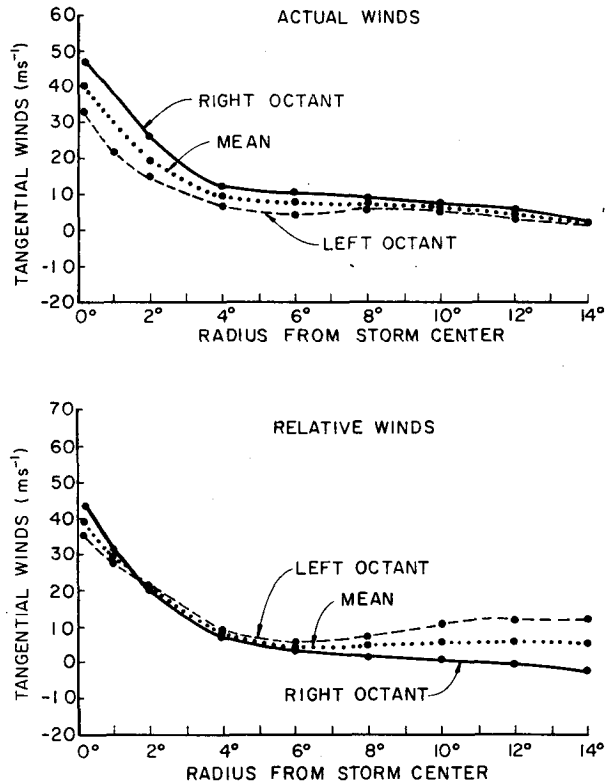

FIG. 7. As in Fig. 6, except for Lat<20°N stratification.

(Shea and Gray, *op. cit.*) from the storm center. In examining the actual winds, it is seen that the asymmetry decreases outward to 10°–12° radius. At 1°–6° radii, most of the right to left side asymmetry is due to the storm motion as can be seen by looking at the relative tangential winds of the right vs left side with the cyclone motion subtracted out. Very few differences between the right and left side are seen in the 1°–6° radial band. At greater radii, the relative tangential winds are stronger in the left octant rather than the right. As Shea and Gray discussed, inside 1° radius a large asymmetry still exists in the relative winds. The important consideration shown here is that between 1°–6° radius, the apparent right-to-left-octant asymmetry is due to the motion of the storm. It is the storm's dynamics imposed upon the normal environmental horizontal height gradient which results in the asymmetry.

b. Normal and parallel wind components of surrounding flow

Figs. 8 and 9 depict the mean normal wind component (V_{NR}) for the single bands through the atmosphere in the relative system (MOTROT) for the two latitude stratifications. For depiction purposes, the radial bands are indicated by a single average radius, i.e., 2° represents the 1°–3° radial band, etc. The zero line indicates that the surrounding wind is directed only along the storm direction of motion. Positive values indicate that the storm is moving to the left of the mean winds, while negative values indicate a storm movement to the right of the mean winds. At the majority of the levels it is apparent that the composite storm is moving to the left of the surrounding mean winds. Similar results are obtained for the other 9 stratifications.

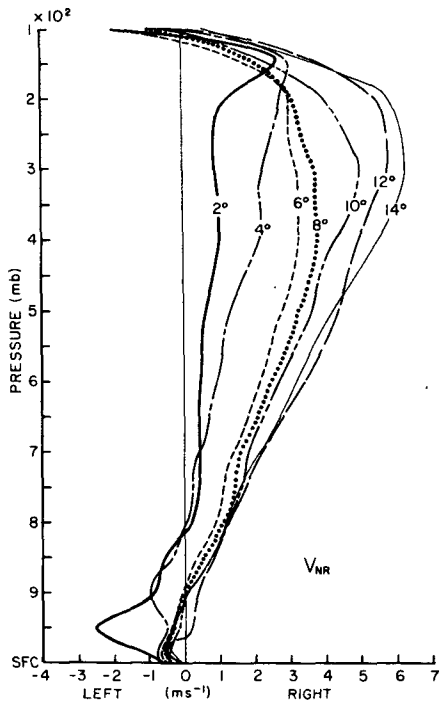

FIG. 8. Relative wind component vector normal (V_{NR}) to the storm motion vector for the various radial band averages and levels for the Lat>20°N stratification.

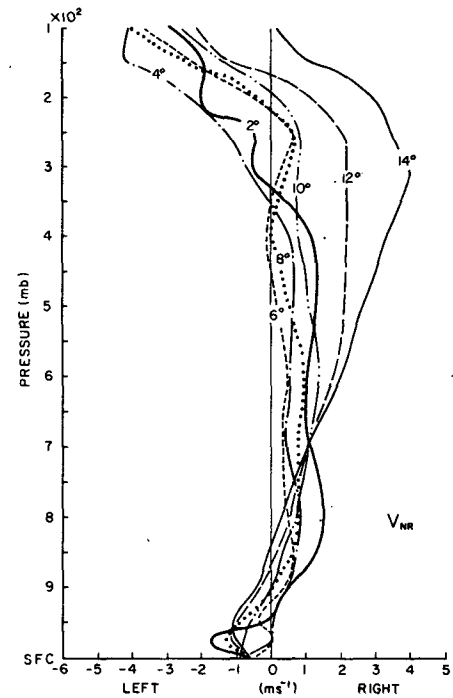

FIG. 9. As in Fig. 8, except for the Lat<20°N stratification.

Figs. 10 and 11 depict the parallel wind component (V_{LR}) for the single levels in the MOTROT system. Positive values indicate that the surrounding winds are moving faster than the storm, while negative values indicate that the component of the surrounding wind along the direction of the storm motion is less than the storm motion. Except at close-in radii, the majority of the points show that the mean storm motion is greater than the mean surrounding flow. Again, similar results are obtained for the nine other stratifications. Thus, at a majority of radii and levels, tropical cyclones are propagating faster than the mean surrounding flow field. The consistency of storm movement in relation to the surrounding wind is evident.

c. Horizontal radial band vectors

Figs. 12 and 13 portray the vector addition of the V_{NR} and V_{LR} relative component vectors for the individual bands at 700 mb. As above, the radial bands are indicated by a single average radius. In essence, these figures depict the individual band's average wind relative to the storm. It is seen that

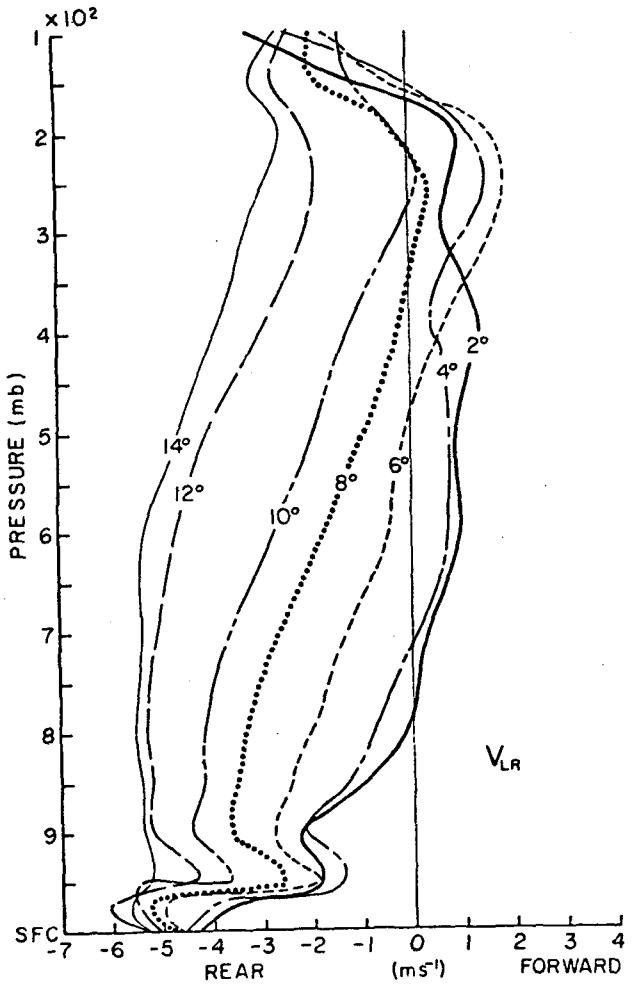

FIG. 10. Relative wind component vector parallel (V_{LR}) to the storm motion vector for the various radial band averages and levels for the Lat>20°N stratification.

the individual band averages of the mean surrounding wind move from the front left quadrant to the right rear quadrant of the composite storm. Thus, the total vector for the band indicates that the storms are propagating faster and moving to the left of the mean wind for each radial band at 700 mb.

d. Storm motion vs actual surrounding mean wind direction and speed (horizontal multiple radial bands)

Using actual winds (ROT), the composite data were investigated for a relationship between the storm motion (direction and speed) and the surrounding wind flow. Data for 21 (1°–5°, 1°–7°, 1°–9°, ..., 13°–15°) multiple bands were examined at the various pressure levels. The composited data were examined separately for a cyclone/surrounding wind direction relationship and a cyclone/surrounding wind speed relationship.

For the directional relationship, each of the 13 stratifications were examined comparing the mean wind direction at the various levels with the mean direction of storm movement for each stratification. The most consistent finding for a directional relationship was found to be the 1°–7° radial band at 500 mb as shown in Fig. 14. Shown are the three mean storm directions (solid lines) for the three direction stratifications (A, B, C). The dashed lines are the mean surrounding wind direction for each of the cases at 500 mb (1°–7° radius). It is seen that the mean storm deviates an average of 16° to the left of the mean winds at this level for the three stratifications. As stated above, this level represents the best consistency for all the stratifications. Consistency refers to the smallest range of the angle between the storm direction and the mean surrounding flow that was found for all 13 stratifications. The standard deviation of these differences for the 1°–7° band direction is 3.4°. Comparisons with other bands are shown later. The difference between the 1°–7° 500 mb storm direction

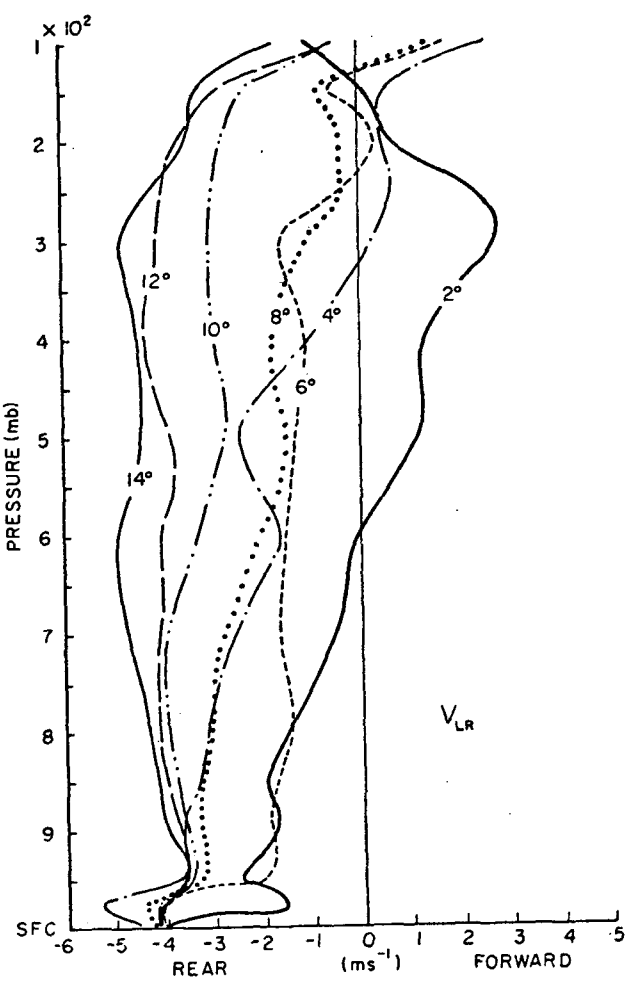

FIG. 11. As in Fig. 10, except for the Lat<20°N stratification.

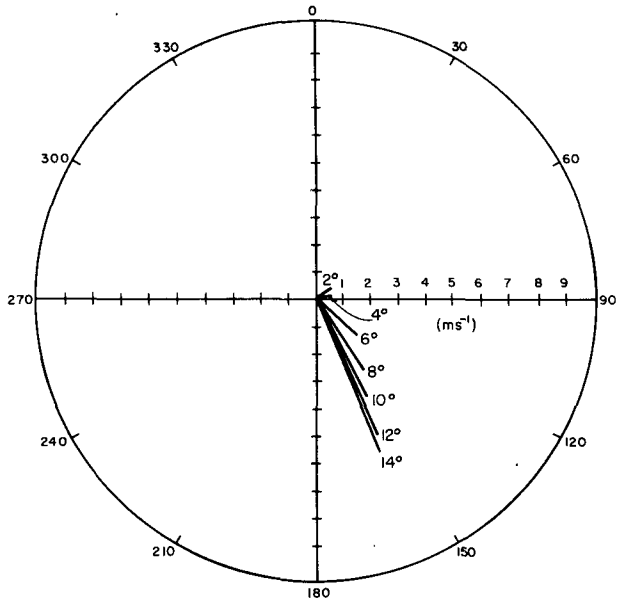

FIG. 12. 700 mb horizontal radial band mean vectors (MOTROT). This depicts the surrounding flow relative winds which blow from the front left quadrant to the rear right quadrant. Lat>20°N stratification.

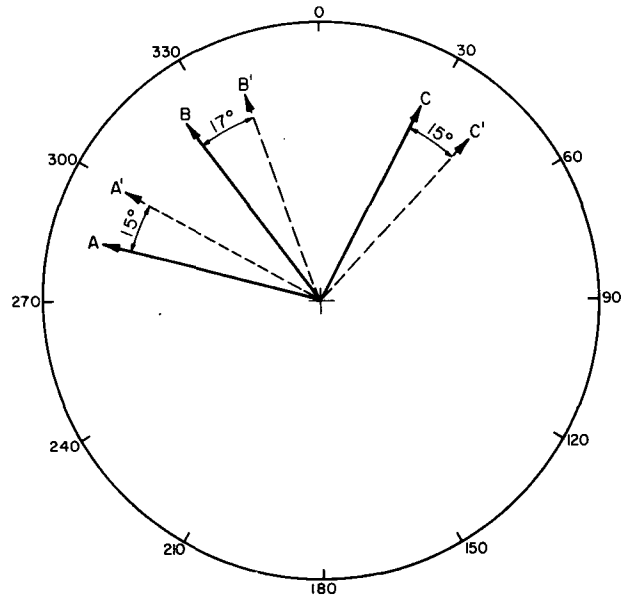

FIG. 14. Relationship between the mean storm direction and the surrounding wind flow for three direction stratifications (horizontal multiple radial band).

and surrounding wind direction angle ranged from 12° to 23° for all 13 stratifications.

Fig. 15 depicts the same relationship for the speed and intensity stratifications. Table 2 summarizes the results for all 13 stratifications. As previously stated, the storms are moving to the left of the mean flow. However, an empirical relationship is now seen as the storms are deviating about ~15°–18° to the left of the mean flow (1°–7° radius at 500 mb) regardless of the storms' latitude, direction of motion, speed, intensity or intensity change.

For the storm speed/surrounding flow relationship, the 13 stratifications were again examined at all levels for a relation between the mean storm speed (S) of each stratification and the surrounding wind speed (W) in the direction of the storm motion. The ratio of

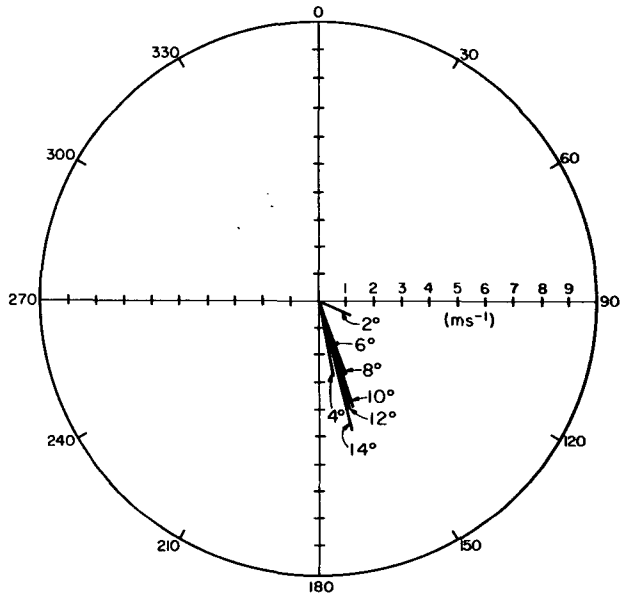

FIG. 13. As in Fig. 12, except for the Lat<20°N stratification.

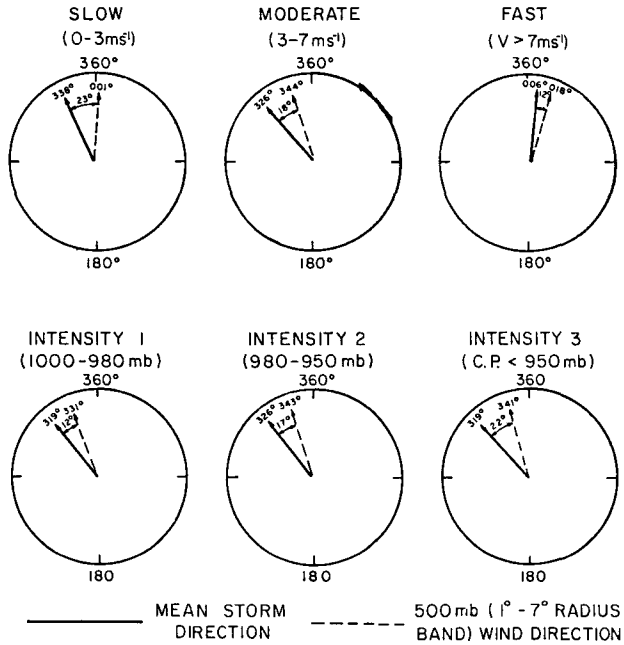

FIG. 15. Relationship between the mean storm direction and the surrounding wind flow for speed and intensity stratifications (horizontal multiple radial band).

TABLE 2. Horizontal multiple radial band summary for 1°–7° band.

Stratification	Mean Storm Direction	Mean 1°–7° Surrounding Wind Direction at 500 mb	Storm Deviation from Surrounding Wind (L=Left)	Mean Storm Speed (ms^{-1})	Mean 1°–7° Surrounding Wind Speed at 700 mb (ms^{-1})	Ratio Storm Speed/Surrounding 1–7° Wind Speed
Latitude						
Latitude >20°N	352°	010°	18°L	5.61	5.06	1.11
Latitude <20°N	300°	314°	14°L	5.05	4.23	1.19
Speed						
Slow Storm Speed 0–3 ms^{-1}	338°	001°	23°L	2.43	2.19	1.11
Moderate Storm Speed 3–7 ms^{-1}	326°	344°	18°L	5.19	4.37	1.19
Fast Storm Speed >7 ms^{-1}	006°	018°	12°L	10.12	8.71	1.16
Direction						
Direction A 250° < Dir. ≤ 310°	285°	300°	15°L	6.16	4.96	1.24
Direction B 310° < Dir. ≤ 350°	324°	341°	17°L	5.32	4.39	1.21
Direction C 350° < Dir. ≤ 060°	027°	042°	15°L	7.08	6.59	1.07
Intensity						
Intensity 1 1000mb ≥ C.P.> 980mb	319°	331°	12°L	4.87	4.07	1.20
Intensity 2 980mb ≥ C.P. > 950mb	326°	343°	17°L	5.03	4.22	1.19
Intensity 3 C.P. ≤ 950mb	319°	341°	22°L	5.17	4.34	1.19
Intensity Change						
Deepening Storms	304°	317°	13°L	4.89	4.31	1.13
Filling Storms	360°	017°	17°L	5.69	5.13	1.11
			Mean: 16.4°L			Mean: 1.16
			Standard Deviation: 3.4°			Standard Deviation: 0.05

the mean storm speed and the mean wind speed (S/W) was calculated for the various levels in the atmosphere. The most consistent results were found at the 700 mb level for the 1°–7° radial band. For this band, the average ratio of the storm speed to the mean surrounding flow in the direction of motion is 1.16. The storm speed to surrounding wind speed ratio ranged from 1.07 to 1.24 with a standard deviation of 0.05. These relationships are depicted in Figs. 16 and 17, and are summarized in Table 2.

The above two findings regarding the relationship of the storm motion and the environmental wind direction and speed statistically verify, for the western North Pacific area, the "steering" concept for tropical storms. Storm movement is, on the average, directly related to the storm's surrounding flow. The composited data indicate that the mean storm moves about 16° to the left of the mean surrounding flow for the 1°–7° radial band at 500 mb, while the ratio of the storm speed to the mean surrounding flow in the direction of the storm motion (1°–7° radius at 700 mb) is 1.16. As stated previously, the above two findings represent the most consistent findings. Other annular bands show similar relationships but with larger deviations.

Table 3 depicts storm direction deviation from the surrounding winds for various multiple radial bands and stratifications. Table 4 shows the ratio of the storm speeds to the surrounding wind speeds for the same multiple bands. Notice that for the larger bands and for the outside bands, the deviations are larger. As the cyclones are often located at the southwestern edge of a subtropical anticyclone, the flow at large radii to the north and west will show more southerly components. This will cause the surrounding flow to be more to the right of the cyclone motion.

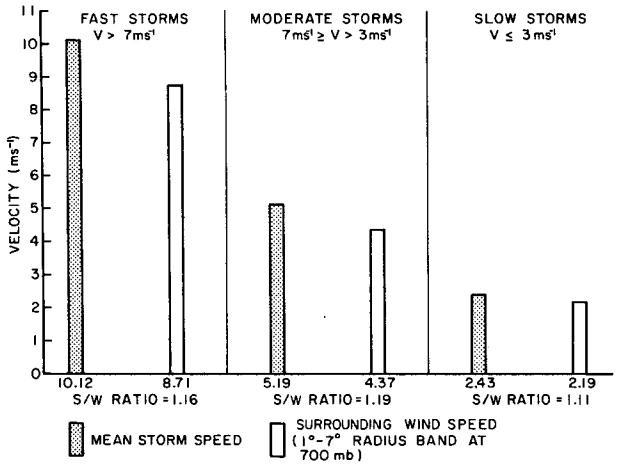

FIG. 16. Relationship between the mean storm speed and the surrounding wind component along the direction of motion for the three speed stratifications (horizontal multiple radial band).

e. Comparison of composite wind components vs calculated geostrophic components

From the composite height data, the geostrophic components of the wind were calculated inside 7° radius. Tables 5 and 6 depict the comparison of the composited wind components with the geostrophic wind components at 700 and 500 mb for all 13 stratifications. At 700 mb the mean normal geostrophic minus actual wind component difference is $\sim$0.1 m s^{-1} while the parallel component mean difference is $\sim$0.6 m s^{-1}. The ratio of actual to geostrophic parallel component for all 13 stratifications is $\sim$0.9, indicating good agreement. At 500 mb, the mean normal component difference is $\sim$0.4 m s^{-1}, the mean parallel component difference is 1.1 m s^{-1}, and the actual/geostrophic parallel component ratio is again $\sim$0.9. This shows a close relation between the actual and geostrophic winds.

Considering the possible influence of the storm's changing acceleration and cumulus convection in upsetting the wind-height relationship, these results are better than expected. In essence, these relationships show that the geostrophic height fields fit almost as well as the actual winds. Because of the good correlation between winds and height, it might be possible in operational analysis to substitute winds for heights or heights for winds depending on which measurement is available.

5. Discussion

These results appear to verify the compositing philosophy. Thus, the inherent errors and unrepresentative sampling by the individual rawinsonde reports must be largely random and mostly average themselves out in the statistical average. This is very encouraging for future studies of synoptic and mesoscale weather systems and is a major finding of this paper. The past rawinsonde network cannot be expanded, but the massive statistical averaging of past data sets can be accomplished with the new computer techniques. Thus it appears that one can substitute time resolution for space resolution for specific types of weather systems.

It has been shown in a statistical sense that tropical cyclone motion is well related to the surrounding wind and height fields. Thus the general concept of a steering flow seems, on the average, to be quite valid. This steering concept has been basically accepted and applied when possible by forecasters for a number of years, but up to now, little or no quantitative verification of this steering hypothesis has been provided. Tropical cyclone direction seems to be very well related to the mean 1°–7° radius 500 mb surrounding wind direction while cyclone speed is best related to the 1°–7° radius surrounding wind speed. In the statistical average, a close relationship exists between the wind and the height fields.

As seen from the results, the surrounding flow appears to dictate the storm motion very well, regardless of storm latitude, speed, direction, intensity and intensity change. Thus in the statistical sense it appears that the structure of tropical cyclones such as the inner convective activity is not a primary factor in influencing storm movement. This is substantiated by the same consistent motion-surrounding flow relations found for the separate stratifications. Thus in the statistical average it appears that variations in the eyewall and inner convection seem to have little or no

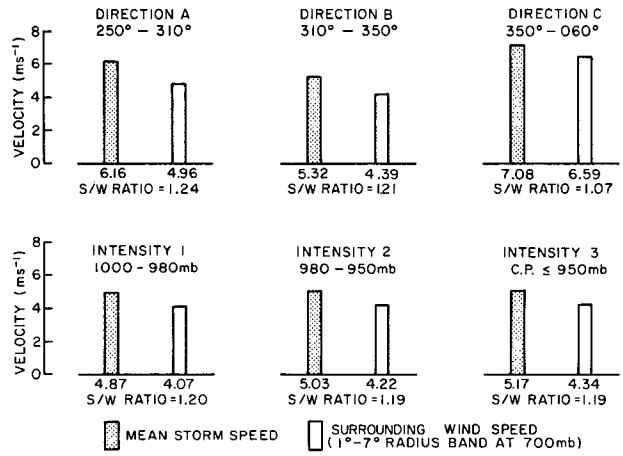

FIG. 17. Relationship between the mean storm speed and the surrounding wind component along the direction of motion for the direction and intensity stratifications (horizontal multiple radial band).

TABLE 3. Direction comparisons for various multiple bands.

Stratification	Storm Deviation from Mean Surrounding Wind (500 mb)				
	1° - 7°	1° - 9°	1°-11°	1°-13°	5° - 9°
Lat > 20°N	18°L	24°L	30°L	40°L	30°L
Lat < 20°N	14°L	12°L	15°L	24°L	7°L
Slow	23°L	31°L	37°L	48°L	39°L
Moderate	18°L	25°L	33°L	44°L	32°L
Fast	12°L	14°L	17°L	21°L	19°L
Direction A	15°L	18°L	22°L	32°L	20°L
Direction B	17°L	19°L	25°L	36°L	19°L
Direction C	15°L	21°L	25°L	32°L	23°L
Intensity 1	12°L	15°L	20°L	23°L	18°L
Intensity 2	17°L	22°L	28°L	37°L	25°L
Intensity 3	22°L	15°L	20°L	38°L	23°L
Deepening	13°L	22°L	22°L	20°L	13°L
Filling	17°L	26°L	13°L	29°L	10°L
Mean:	16.4°	20.3°L	23.6°L	32.6°L	21.3°L
σ :	3.4°	5.5°	7.0°	8.9°	8.9°

L : Storm direction to Left of mean surrounding wind direction

TABLE 4. Speed comparisons for various multiple bands.

Stratification	Storm Speed/Surrounding Wind Speed Ratio (S/W) at 700 mb				
	1° - 7°	1° -9°	1°-11°	1°-13°	5° - 9°
Lat >20°N	1.11	1.32	1.61	2.12	1.54
Lat <20°N	1.19	1.74	2.22	2.76	1.86
Slow	1.11	1.42	1.69	2.78	1.56
Moderate	1.19	1.40	1.75	2.32	1.47
Fast	1.16	1.39	1.67	2.08	1.47
Direction A	1.24	1.25	1.50	1.86	1.48
Direction B	1.21	1.13	1.37	1.69	1.33
Direction C	1.07	1.96	2.36	3.45	2.43
Intensity 1	1.20	1.38	1.62	1.96	1.56
Intensity 2	1.19	1.42	1.79	2.38	1.69
Intensity 3	1.19	1.57	2.03	2.66	2.76
Deepening	1.19	1.38	2.06	2.50	1.84
Filling	1.11	1.24	1.33	2.04	1.25
Mean:	1.16	1.43	1.77	2.35	1.71
σ :	.05	.22	.32	.48	.43

TABLE 5. 700 mb comparison of composite wind components vs calculated geostrophic components.

Stratification	Normal component inside 7° radius ($m\ s^{-1}$) Actual wind composite	Geostrophic wind composite	Difference	Parallel component inside 7° radius ($m\ s^{-1}$) Actual wind composite	Geostrophic wind composite	Difference	Ratio actual to geostrophic
1. Lat>20°N	+0.96	+0.46	+0.50	+5.01	+6.20	−1.19	0.81
2. Lat<20°N	+0.68	+1.30	−0.62	+3.30	+3.54	−0.24	0.93
3. Slow	+0.33	+0.81	−0.48	+2.17	+3.65	−1.48	0.59
4. Moderate	+0.87	+1.62	−0.75	+4.33	+5.27	−0.94	0.82
5. Fast	+1.93	+1.05	+0.88	+8.64	+8.89	−0.25	0.97
6. Direction A	+1.41	+1.12	+0.29	+3.96	+3.03	+0.93	1.31
7. Direction B	+0.76	+0.54	+0.22	+5.33	+6.08	−0.75	0.87
8. Direction C	+1.11	+0.23	+0.88	+5.53	+7.00	−0.47	0.93
9. Intensity 1	+1.17	+1.27	−0.10	+4.04	+4.09	−0.05	0.99
10. Intensity 2	+1.38	+1.83	−0.45	+4.19	+5.51	−1.32	0.76
11. Intensity 3	+0.99	+1.69	−0.70	+4.10	+4.09	+0.01	1.00
12. Deepening	+1.30	+0.82	+0.48	+4.15	+3.92	+0.23	1.06
13. Filling	+1.51	+0.89	+0.62	+5.39	+7.09	−1.70	0.76
Mean	+1.11	+1.05	+0.06	+4.70	+5.26	−0.56	0.91

contribution to the steering flow and the resulting cyclone motion.

If the surrounding flow could be better monitored, the information in this paper might be used to improve cyclone forecasting. Furthermore, for critical forecasts, such as when a major storm is threatening a large population area, aircraft could fly around the cyclone at 5° to 7° radius and monitor the surrounding steering flow and determine how this changes. If there is a lag in response of the cyclone center motion to the winds or heights at outer radii, then some forecasting skills may be derived by monitoring the outer fields. If the cyclone center moves in response to the outer circulation fields, then cyclone motion changes might first be detected in the outer radii fields.

To what extent can the surrounding flow field be used as a predictor? The next logical step in this research will be to investigate the possible lag in response of the cyclone center motion to the outer flow fields. This requires comparing cyclone center motion changes with the prior 12–24 h surrounding field changes. Future tropical cyclone motion research

TABLE 6. 500 mb comparison of composite wind components vs calculated geostrophic components.

Stratification	Normal component inside 7° radius ($m\ s^{-1}$) Actual wind composite	Geostrophic wind composite	Difference	Parallel component inside 7° radius ($m\ s^{-1}$) Actual wind composite	Geostrophic wind composite	Difference	Ratio actual to geostrophic
1. Lat>20°N	+1.92	+1.03	+0.89	+5.91	+7.11	−1.20	0.83
2. Lat<20°N	+0.95	+1.30	−0.35	+3.82	+2.98	+0.84	1.28
3. Slow	+1.08	+0.54	+0.54	+1.92	+3.24	−1.32	0.59
4. Moderate	+2.80	+1.89	−0.09	+4.53	+7.16	−2.63	0.63
5. Fast	+2.15	+0.52	+1.63	+11.95	+13.61	−1.66	0.88
6. Direction A	+1.18	+0.16	+1.02	+4.36	+4.78	−0.42	0.91
7. Direction B	+1.39	+0.00	+1.39	+4.43	+6.22	−1.79	0.71
8. Direction C	+2.45	+1.95	+0.50	+8.56	+10.67	−2.11	0.80
9. Intensity 1	+1.03	+0.85	+0.18	+4.73	+5.50	−0.77	0.86
10. Intensity 2	+1.96	+4.09	−2.13	+5.01	+5.36	−0.35	0.93
11. Intensity 3	+1.99	+1.69	+0.30	+3.61	+5.36	−1.75	0.67
12. Deepening	+1.15	+0.15	+1.00	+4.58	+5.00	−0.42	0.92
13. Filling	+2.49	+1.63	+0.85	+6.72	+7.26	−0.54	0.93
Mean	+1.66	+1.22	+0.44	+5.39	+6.48	−1.09	0.91

will be directed to these ends. For more information on this research, the reader is referred to the more detailed project report of George (1975).

Acknowledgments. This study was made possible by the special computer programming expertise of Messrs. Edwin Buzzell and Charles Solomon. Gratitude is extended to Mr. William M. Frank and Major Charles P. Arnold for enlightening discussions. Mrs. Barbara Brumit and Ms. Genevra Metcalf assisted in the data reduction and manuscript preparation.

This research was accomplished while the first author was enrolled in the U. S. Air Force Institute of Technology (AFIT) meteorology program at Colorado State University, and has largely been supported by NOAA Grant 04-5-022-14. The punching of the Japanese rawinsonde data was accomplished through arrangement with the U. S. Navy Environmental Prediction Research Facility.

REFERENCES

George, J. E., 1975: Tropical cyclone motion and surrounding parameter relationships. Atmos. Sci. Res. Pap. No. 241, Colorado State University, 105 pp.

Ruprecht, E., and W. M. Gray, 1974: Analysis of satellite-observed tropical cloud clusters. Atmos. Sci. Res. Pap. No. 219, Colorado State University, 91 pp.

Shea, D. J., and W. M. Gray, 1973: The hurricane's inner core region, I: Symmetric and asymmetric structure. *J. Atmos. Sci.*, **30**, 1544–1564.

Williams, K. T., and W. M. Gray, 1973: Statistical analysis of satellite-observed trade wind cloud clusters in the western north Pacific. *Tellus*, **25**, 313–336.

Selective Bibliography of Tropical Cyclone Forecasting Methods

Gray, W. M., 1971: A climatology of tropical cyclones and disturbances of the western Pacific with a suggested theory for their genesis/maintenance. NAVWEARSCHFAC Tech. Pap. No. 19–70, Monterey, Calif., 225 pp.

Hope, J. R., and C. J. Neumann, 1970: An operational technique for relating the movement of existing tropical cyclones to past tracks. *Mon. Wea. Rev.*, **98**, 925–933.

Jarrell, J. D., and W. L. Somervell, 1970: A computer technique for using typhoon analogs as a forecast aid. NAVWEARSCHFAC Tech. Pap. No. 6–70, Norfolk, Va.

Miller, B. I., and P. P. Chase, 1966: Prediction of hurricane motion by statistical methods. *Mon. Wea. Rev.*, **94**, 399–406.

——, E. C. Hill and P. P. Chase, 1968: A revised technique for forecasting hurricane movement by statistical methods. *Mon. Wea. Rev.*, **96**, 540–548.

——, P. P. Chase and B. R. Jarvinen, 1972: Numerical prediction of tropical weather systems. *Mon. Wea. Rev.*, **100**, 825–835.

Neumann, C. J., 1972: An alternate to the Hurran tropical cyclone forecast system. Tech. Memo. NWS SR-62, National Weather Service, Southern Region, Miami, Fla.

——, J. R. Hope and B. I. Miller, 1972: A statistical method of combining synoptic and empirical tropical cyclone prediction systems. Tech. Memo. NWS SR-63, National Weather Service, Southern Region, Miami, Fla.

——, and M. B. Lawrence, 1973: Statistical-dynamical prediction of tropical cyclone motion (NHC-73). Tech. Memo. NWS SR-69, National Weather Service, Southern Region, Miami, Fla.

Renard, R. J. *et al.*, 1973: Forecasting the motion of north Atlantic tropical cyclones by the objective MOHATT scheme. *Mon. Wea. Rev.*, **101**, 206–214.

Sanders, F., 1970: Dynamic forecasting of tropical storm tracks. *Trans. N. Y. Acad. Sci.*, **32**, 495–508.

——, and R. H. Burpee, 1968: Experiments in barotropic hurricane track forecasting. *J. Appl. Meteor.*, **7**, 313–323.